Available online at www.sciencedirect.com
ScienceDirect
Journal of Power Sources 180 (2008) 1–14
JOURNAL OF POWER SOURCES
www.elsevier.com/locate/jpowsour

Review

A review of the main parameters influencing long-term performance and durability of PEM fuel cells

Wolfgang Schmittinger, Ardalan Vahidi *

Department of Mechanical Engineering, Clemson University, Clemson, SC 29634-0921, USA

Received 11 November 2007; received in revised form 13 January 2008; accepted 22 January 2008
Available online 9 February 2008

Abstract

This paper presents an overview of issues affecting the life and the long-term performance of proton exchange membrane fuel cells based on a survey of existing literature. We hope that this brief overview provides the engineers and researchers in the field with a perspective of the important issues that should be addressed to extend the life of next-generation fuel cells. Causes and fundamental mechanisms of cell degradation and their influence on long-term performance of fuel cells are discussed. Current research shows that main causes of short life and performance degradation are poor water management, fuel and oxidant starvation, corrosion and chemical reactions of cell components. Poor water management can cause dehydration or flooding, operation under dehydrated condition could damage the membrane whereas flooding facilitates corrosion of the electrodes, the catalyst layers, the gas diffusion media and the membrane. Corrosion products and impurities from outside can poison the cell. Thermal management is particularly important when the fuel cell is operated at sub-zero and elevated temperatures and is key at cold start-ups as well as when subjected to freezing conditions.

Keywords: Fuel cells; Durability; Long-term performance; Lifetime

Contents

* Corresponding author. Tel.: +1 864 656 4718; fax: +1 864 656 7299.
E-mail addresses: w.schmittinger@arcor.de (W. Schmittinger), avahidi@clemson.edu (A. Vahidi).

0378-7753/$ – see front matter © 2008 Elsevier B.V. All rights reserved.
doi:10.1016/j.jpowsour.2008.01.070

1. Introduction

The relatively short life of polymer electrolyte membrane (PEM) fuel cells is a significant barrier to their commercialization in stationary and mobile applications. A longer life span for fuel cell components should be achieved to ensure high reliability, low maintenance costs and to justify fuel cells as economical alternative energy systems. The lifetime target of the Department of Energy (DOE) by 2010 requires PEM fuel cells to achieve 5000 h for mobile and 40,000 h for stationary applications [1–3]. Currently, the lifetime targets can only be met under best laboratory conditions. For example, Mercedes–Benz claims a lifetime of above 2000 h without performance degradation for their current fuel cell stacks operated in test-vehicles all over the world [4].

To date long-term performance and durability of fuel cells are difficult to quantify because not all degradation mechanisms of the various fuel cell components are completely understood. More research on individual components is needed to fully understand the interactions influencing the life of the stack [1,5–8]. The voltage degradation rate is normally a good indicator of a fuel cell state of health. It is usually in the range of 1–10 $\mu V\,h^{-1}$ [5], but can also exceed these values due to harsh and extreme operating conditions. Table 1, gives an overview of degradation rates determined in long-term durability tests by various researchers together with further information on testing conditions whenever available. This paper integrates the result of existing but scattered research in the hope to provide a quick overview of the main parameters known to influence a PEM fuel cell's performance and life. We discuss the fundamental cell degradation mechanisms and their influence on long-term performance and durability. The paper's emphasis is on chemical and resulting mechanical issues rather than on design and assembly impacts. The influence of water management, more specifically the influence of flooding and dehydration on fuel cell life will be presented first. The durability issues due to corrosion, cell contamination and reactant starvation will follow. Finally, thermal management, in particular fuel cell operation at sub-zero and elevated temperatures will be discussed.

2. Influence of water management on fuel cell performance and life

Recent study has shown that water management is of vital importance to ensure stable operation, high efficiency and to maintain the power density of PEM fuel cells in the long run [24–26]. On one hand it is important to keep the membrane humidified for high proton conductivity, because the membrane's conductivity is directly related to its water content [24]. On the other hand accumulation of too much water also impacts performance and lifetime of the fuel cell. Excess water can block the flow channels and the pores of the gas diffusion layer (GDL) and can instantly lead to reactant starvation. Reactant starvation denotes operation of a fuel cell under sub-stoichiometric reaction conditions. Too much water also aggravates other degradation mechanisms such as corrosion and contamination of compo-

Table 1
Results of long-term durability tests under laboratory conditions (steady state)

Authors	Test time (h)	Degradation rate ($\mu V\,h^{-1}$)
Sishtla et al. [9] (reformate fuel, 4 thermal cycles over 1200 h)	5100	6
Washington [10] (Ballard Mk5R)	4700	6
Washington [10] (Ballard Mk6000)	8000	2.2
Nakayama [11]	4000	4.3
Maeda et al. [12] (on reformate fuel)	5000	6
Fowler et al. [13] (non-continuous operation, start-stop cycling, long-term storage, dehydration, flooding)	600	120
Endoh et al. [14]	4000	2
Knights et al. [15] (short stack, methane reformate operation, 0.5 $A\,cm^{-2}$)	13,000	0.5
Scholta et al. [16] (GDL Toray TGP 120, 600 $mA\,cm^{-2}$, T_{stack} = 65–70 °C, H_2, O_2 humidified)	2500	20
Scholta et al. [16] (GDL SIGRACET® SGL-10BB, 300 $mA\,cm^{-2}$, T_{stack} = 55 °C, H_2 = 1.3 bar, dry O_2 = ambient pressure, dry)	2500	60
Cheng et al. [17] (400 $mA\,cm^{-2}$, T_{cell} = 60 °C, H_2 O_2: RH = 100%, ambient pressure)	4000	3.1
Wang et al. [18] (~1.0 $A\,cm^{-2}$, 0.64 V)	1000	54
Lightner [19,20] (first 1000 h steady state, degradation 2 $\mu V\,h^{-1}$; then accelerated cyclic testing)	4000	20
Borup et al. [21,22] (steady-state, T_{cell} = 80 °C, RH_{H_2/O_2} = 75%, gas $press_{H_2/O_2}$ = 15 psig, flow $rate_{H_2/O_2}$ = 1.2/2.0*1.5 $A\,cm^{-2}$ equiv.)	1000	12
Cleghorn et al. [23] (single cell, 800 $mA\,cm^{-2}$, T_{cell} = 70 °C, RH H_2, O_2 100%)	26,300	4–6

nents. The longer the cell is exposed to excess water the stronger is the degradation. Therefore a proper water balance between water formation and water removal is required [25,27]. The water balance depends on the water carried in or formed inside the cell and the water removed out of the cell. Reactant gases, which are pre-humidified or saturated and the oxygen-reduction reaction at the cathode generate water within the cell. Water is removed by evaporation into the gas streams, exiting humidified gases and exiting liquid water.

2.1. Fuel cell flooding

Flooding is the accumulation of excess water and can happen at both the anode and cathode side of the membrane. Fuel cell flooding occurs particularly at the cathode [5]. There is considerable literature on this issue and in particular cathode flooding.

Flooding leads to instant increase in mass transport losses, particularly at the cathode; that is the transport rate of the reactants to the electrocatalyst sites is significantly reduced [5,28]. Water blocks the pores of the GDL which creates a sterical hindrance preventing the reactants to reach the catalysts leading to gas starvation and an immediate drop in cell potential. However, the voltage can be recovered relatively fast by purging the cathode and anode as shown in experiments [29]. Due to the water layer on the GDL surface, its pore size may be reduced. Consequences are dissolution and diffusion of the reactant gas into the liquid water. In addition the gas may be forced to flow through alternative channels which results in a partial pressure decrease across the backing layers [24,27,29]. He et al. [28] correlated partial pressure directly to the flooding level and considered it to be a good indicator for performance. They designed a tool to monitor the flooding level in PEM fuel cells with interdigitated flow fields. However, the authors state that no modification is needed for utilizing the monitoring device for other existing fuel cell designs. There is also a US patent filed by Dipierno and Fronk who claim to have developed a method and a device that monitors the pressure drop across the flow fields to detect and correct flooding of common PEM fuel cells [30]. Fig. 1 shows clearly that cathode flooding has a negative effect on fuel cell performance. Especially at higher current densities (above 0.55 A cm^{-2}) the partial-gas-pressure-drop at the cathode due to flooding increases significantly which results in a considerable cell voltage drop [28]. They show that if the cathode pressure-drop doubles from 1.5 kPa to around 3 kPa, the initial cell voltage of 0.9 V goes down to around one third of its initial value (cell temperature, 51 °C; H_2 flow rate, 2.0 A cm^{-2} equiv.; air flow rate, 2.8 A cm^{-2} equiv., ambient pressure; H_2 temperature, 50 °C; air temperature, 27 °C) [28]. Weber et al. [31] developed a model for determining the water effects in GDLs and coupled it to a membrane model. They show that the fraction of hydrophobic pores, f_{HO} ($f_{HO} = 1 - f_{HI}$, f_{HI} = fraction of hydrophilic pores) of a GDL plays an important role in the maximum power and the limiting (maximum) current in a fuel cell. At low values of f_{HO} (that is high hydrophilicity, hence higher chance of excess water in the GDL) the maximum power is limited due to low values of limiting current, and due to mass transport limitations of oxygen

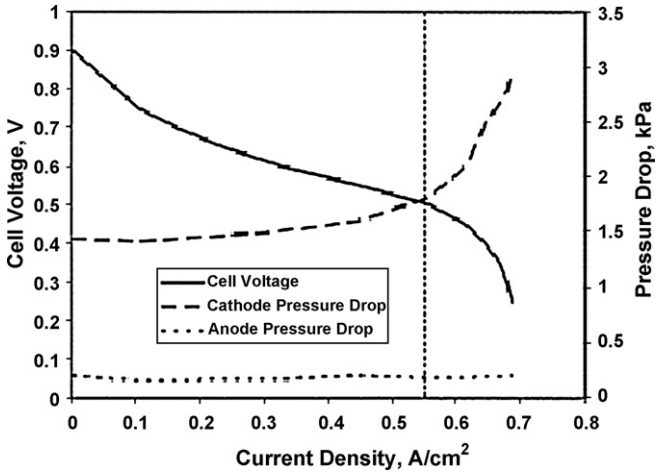

Fig. 1. Effect of cathode flooding on fuel cell performance (cell temperature, 51 °C; H_2 flow rate, 2.0 A cm^{-2} equiv.; air flow rate, 2.8 A cm^{-2} equiv., ambient pressure; H_2 temperature, 50 °C; air temperature, 27 °C). (Reproduced from [28] with permission – copyright© 2003 AIChE).

in the cathode. The optimum value of f_{HO} was determined to be 0.45, where the maximum power (W cm^{-2}) of the cell could be reached. Turhan et al. and Kowal et al. [32,33] (same laboratory, Pennsylvania State University) brought to light that in the case of over-humidified reactants, the water inside the cell increased with decreasing cell pressure, yet for under-humidified inlet conditions the contrary was observed. Kowal et al. also investigated the effect of current on the water level in cells with two different diffusion media materials (paper, cloth), but a clear trend could not be found [33]. However, the two different materials followed the same behavior.

In the long run flooding has a considerable impact on durability. An excess of water accelerates corrosion of the electrodes, the catalyst layers, the gas diffusion media and the membrane [24,29]. Leached impurities either from corroded parts such as the bipolar plates (and from the reactant gases) can be deposited on the catalysts. Hence, ohmic losses increase and the performance of the electrodes decreases. Dissolved catalyst particles and the aforementioned impurities can also be transported in the membrane replacing H^+-ions. Thus, the proton conductivity can be reduced over time, eventually leading to cell failure[34].

2.1.1. Cathode flooding

Three mechanisms contribute to flooding of the cathode, especially at its GDL. (i) Water formation due to the oxygen-reduction reaction generates water. More water is formed when the load or the current density of the fuel cell is increased. (ii) Electro-osmosis under the influence of an applied electric field across the membrane takes place. The electro-osmotic drag causes protons moving through the membrane to pull water molecules from the anode to the cathode. The rate of transported water depends on the humidification level of the membrane and increases with increasing current density [27]. Ngyuen and White [27] have shown that along 10 cm of a flow channel, where the membrane hydration level at the inlet is higher than at the exit, the electro-osmotic drag coefficient at the inlet was around 5 times higher than at the exit. (iii) Saturated or over-humidified

reactant gases as well as liquid water injection also facilitate flooding.

Water removal mechanisms are water back-diffusion to the anode, evaporation, water-vapor diffusion and capillary transport of liquid water through the porous cathode backing layer [28]. Water back-diffusion takes place when the water content of the cathode side of the membrane exceeds that of the anode side [35]. In comparison to other mechanisms, back-diffusion does not contribute much to water removal. Only at low current densities ($<\approx 0.3\,A\,cm^{-2}$) the effect of back-diffusion can exceed electro-osmosis [27]. Water evaporation is facilitated by higher cell temperatures and a higher air flow rate is beneficial to carry water out of the cell. He et al. [28] show that by increasing the cell temperature from 40 to 50 °C the cathode pressure can drop from 3 to 2 kPa and hence the flooding level drops within 15 min (air flow rate, $2.0\,A\,cm^{-2}$; H_2 flow rate, $2.0\,A\,cm^{-2}$; p = ambient pressure; H_2, 43 °C; air, 25 °C). Several factors, caused by a higher temperature contribute to a higher water removal rate. At higher temperatures, water evaporation as well as the volumetric air flow rate (if the mass flow rate of air stays the same) will increase. Also, a decrease in surface tension and viscosity of water makes it easier to flush water out of the cell [28]. Under the same conditions doubling of the air flow rate to $4\,A\,cm^{-2}$ leads to a current density increase from 0.5 to around $0.75\,A\,cm^{-2}$ within 1 h [27]. The capillary transport of water through the porous cathode backing layer to the flow channels also helps reducing the hydration level [28].

2.1.2. Anode flooding

Since the cathode is naturally the water generating electrode, it takes much longer to accumulate water at the anode [36]. Although flooding at the anode happens less often than at the cathode, it can have serious consequences on fuel cell operation; one being fuel starvation with subsequent carbon corrosion in the catalyst layer. Also, due to usually low hydrogen flow rates, liquid water is more likely to stay in the anode [36].

(i) Anode flooding is more likely to happen at low current densities [29]. In experiments carried out by Ge and Wang [36] liquid water at the anode could only be found when operating the cell at low current densities ($0.2\,A\,cm^{-2}$), whereas at high current densities a higher electro-osmotic force reduced the water content at the anode. In addition, lower cell temperatures and hence higher water condensation in the anode channels contribute to anode flooding [36]. Pasaogullari and Wang [11] confirm the statement of Ge and Wang that anode flooding is often observed at low current densities, especially at low reactant flow rates and lower temperatures. At the inlet of the anode, where the proton flux is high, a strong electro-osmotic force drags the water molecules from the anode to the cathode resulting in low water content. At the exit in contrast, where the current density is lower, the water content is higher. Two other (independent) mechanisms also seem to contribute to anode flooding.

(ii) Nguyen and White [27] show that anode flooding can be caused by water back-diffusion from the cathode together with a low hydration state of the fuel gas stream. If the hydration state is not as high as at the cathode in addition to low current densities, water back-diffusion through the GDL to the anode will surpass the electro-osmotic effect. Ge and Wang [36] observed, by using a camera, that water vapor coming from the anode GDL condensed at its surface. However, the water accumulation by condensation did not seem to be much.

(iii) Liquid water injection for cooling and humidification together with moderate cell temperatures (lower evaporation) can be another reason for anode flooding [27,29]. Liquid-water accumulation in the anode by humidification was confirmed by Ge and Wang [36].

2.2. Dehydration of the membrane

Dehydration of the membrane is more likely to occur at the anode side of the membrane. The main factor contributing to dehydrated condition of the membrane is probably poor water management leading to a shortage of water. Dehydrated cell operation leads to instant and long-term degradation. The main consequence of dehydration is drying of the proton-conducting membrane. With decreasing water content the conductivity decreases which leads to higher ionic resistance and higher ohmic losses [5,24,37]. That results in a substantial drop in cell potential and thus a temporary power loss [24,27,35]. Although a temporary drop in voltage can usually be recovered by humidification, dry cell operation over a long time can cause serious and irreversible damage to the membrane. The recovery time depends on the membrane thickness and the water diffusion coefficient [24,35]. Sone et al. [37] measured the conductivity for Nafion 117 membranes in terms of relative humidities (RH) with the AC impedance method (Table 2). Fig. 2 shows an experiment performed by Le Canut et al. [24] in which a cell was exposed to drying conditions for about 12 min. In this time period the initial cell voltage of around 0.8 V (current density = $0.1\,A\,cm^{-2}$) dropped to about 0.75 V. After 15–20 min of rehumidification the initial value could be reached again. Data of Büchi and Srinivasan [38] collected in lifetests under zero external humidification show long-term MEA performance degradation. In 1200 h of operation (observed in the interval from 150 to 1350 h of operation) the current density dropped from 170 to 130 $mA\,cm^{-2}$ at a constant potential of 0.61 V.

Anode dehydration is expected to be more serious at the inlet of the cell. That can be explained by the higher water back-diffusion to the anode at the bottom of the cell. Since the hydration state at the exit of the cathode is higher, caused by exit-

Table 2
Conductivity ($S\,cm^{-1}$) at different relative humidities [%] for E- and N-form Nafion 117 membranes (E-form: no heat-treatment, N-form: heat treatment at 85 °C and 105 °C) [37]

		RH (%)		
		20	60	100
Proton conductivity ($S\,cm^{-1}$)	E-form	$\approx 2\times10^{-3}$	$\approx 2\times10^{-2}$	$\approx 7\times10^{-2}$
	N-form	$\approx 3\times10^{-4}$	$\approx 8\times10^{-3}$	$\approx 5\times10^{-2}$

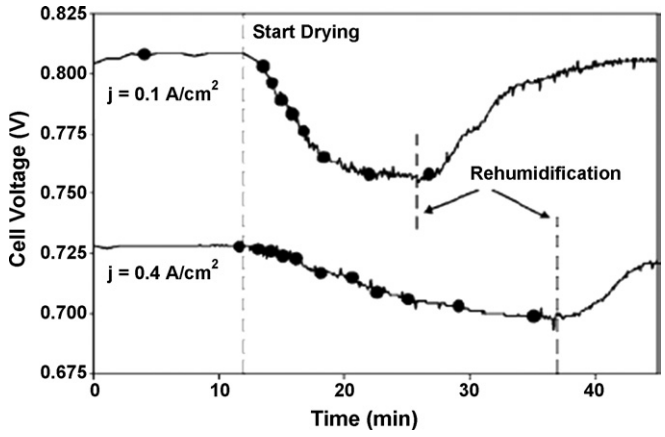

Fig. 2. Cell potential with time for cell dehydration and re-humidification [24]. (Reproduced by permission of ECS – The Electrochemical Society).

ing water, the back-diffusion is higher as well [39]. Moreover, under dehydrated condition the membrane pores shrink which leads again to lower back-diffusion rates. During operation this effect can be aggravated by a poor thermal management [27].

According to [40] when membranes are exposed to dry conditions over a longer time, they can become brittle and develop crazes or cracks. This causes gas crossover and therefore uncontrolled reaction of H_2 and O_2 which results in formation of hot spots. Hot spots are high chemically active areas on the membrane caused by the exothermic reaction of H_2 and O_2. This in turn causes pinholes leading to more gas crossover. Once this process is initiated a "destructive cycle" of increasing gas crossover and pinhole production is established [41]. This procedure is explained in depth under the topic "4.3 Corrosion and Mechanical Degradation of the Membrane". Generally, the drier the operating conditions, the shorter will be the life of the cell [5]. We were not able to find conclusive works that quantify the influence of dry operation on the life of the stack.

Three main reasons for dehydration can be given: (i) sufficient humidification cannot be maintained when feeding the cell with low-humidified or dry reactant gas streams. Water formation reaction at the cathode alone is not able to compensate the lack of water; (ii) additionally, evaporation of water and subsequent vapor removal through the flow channels, mainly at higher cell operating temperatures can play a role [42]; (iii) electro-osmosis can also lead to dehydrated condition at the anode. As mentioned above, the electro-osmotic force is strong when a high electric field at high current densities exists. It has been observed that at high current densities the water replenishment by back-diffusion is not sufficient to keep the anode side of the membrane wet [43–45]. For example Wang and Wang [35] show that during a step increase of the current density the electro-osmotic force will immediately pull water molecules from the anode to the cathode.

3. Degradation of the electrodes/electrocatalyst, membrane, gas diffusion layer and bipolar plates

In PEM fuel cells corrosion of the electrocatalyst layers, the membrane and the GDL is detrimental to fuel cell life and among the important degradation mechanisms [46]. Depending on the current and the long-term operating conditions of the fuel cell, the extent of performance and durability degradation varies. In general, the longer the fuel cell stack is operated in transient or cyclic condition, the stronger is the corrosion and therefore the deterioration [7,46–50].

3.1. Corrosion of the electrodes/electrocatalyst

Corrosion of the electrocatalyst layers is one fundamental mechanism that strongly influences performance in the long run and is a major hurdle in commercialization of PEM fuel cells [7]. Corrosion of the catalyst is frequently addressed in the existing literature and is one of the better understood degradation mechanisms of PEM fuel cells [5,7,46].

The material used for catalysts for both anode and cathode is usually platinum (Pt) or a platinum alloy with particles of nanometer size. In most designs of today's PEMFC the basic structure of the electrodes is similar; often anode and cathode are exactly the same. Frequently carbon paper or cloth builds the basic mechanical structure of the electrode. Platinum catalyst formed into very small particles is applied on the carbon surface. Since the carbon paper also facilitates the diffusion of the reactants onto the catalyst it is known as the GDL [47,51,52].

Corrosion of the platinum catalyst means the loss and change in structure and distribution of the platinum on the carbon support accompanied by a decrease in electrochemical active surface area (ECSA) of the electrode [5,7,46]. Corrosion of the carbon support indicates the loss or dissolution of carbon particles along with Pt-particles bound on their surface [5].

With the presence of water and especially at higher relative humidities, corrosion of the electrodes, mainly at the cathode occurs [46]. Potential cycling, the number of cycles, the cell temperature and the humidification level are the most important factors contributing to corrosion. Consequences are a lower cell output voltage [5,7,46].

3.1.1. Cathode corrosion

In various experiments reported in different papers the ECSA of the Pt-catalyst was measured and it could be shown that it decreased with time [7,46,47,52–54]. The loss of ECSA can be explained by redistribution (agglomeration/sintering) of initially small narrow and uniformly dispersed Pt-particles to form larger particles which are then distributed more widely [46,54]. The order of the particle-size growth is in the range of nanometers. Also oxidation on the surface can occur [5]. The work of Borup et al. [7] shows that the loss of ECSA can be directly correlated to particle-redistribution. The stronger the particle growth the less will be the ECSA and eventually the output cell voltage. Additionally, activation losses will increase in this process. Borup et al. also observed that during particle redistribution there is no net loss of platinum over time. However, other work has shown that together with redistribution (and dissolution of carbon) whole Pt-particles can fall off and are either lost or diffused into the membrane or the GDL, although not very often [18,55]. The redistribution of the Platinum particles and hence the loss of ECSA is dependent on the long run operating conditions of the cell:

Table 3
Potential cycling effect on the electrochemical active surface area (ECSA) [7]

# of potential cycles	% initial ECSA (0.1–0.75 V)	% initial ECSA (0.1–1.2 V)
300	96	60
900	90	23
1500	83	11

Table 4
Pt-particle size (nm) after cycling from 0.1 to 0.96 V as a function of relative humidity and cycling temperature [7]

RH (%)	10	50	100
Pt-particle size (nm)	2.6	3.2	3.3
Temperature (°C)	60	100	120
Pt-particle size (nm)	2.8	4.1	4.8

(i) Cell potential cycling is one of the most important factors contributing to platinum agglomeration and/or oxidation and hence to a decrease in ECSA. Table 3 shows that with the number of cycles, the lifetime of the catalyst and cell potentials strongly go down. For instance, in simulated drive cycle tests of Borup et al. [46] a 10% decrease of the ECSA could be observed after operating a cell for 850 h under 100% RH (20-min cycles, total 2550 cycles). Other experiments of Borup et al. show a loss of the ECSA of around 40% after 1500 potential cycles from 0.1 to 1.0 V [7].

During cycling the Pt-particle size grows depending on the cell potential and faster than during constant potential operation. In general, higher potential levels accelerate cell degradation. Agglomeration can also be noticed during constant cell voltages, but it is not as strong. For instance, the particle-size can increase up to 8 nm after 1500 cycles from 0.1 to 1.2 V (cell temperature, 80 °C; H_2 RH 226%, air RH 100%) [7]. Wilson et al. [56] have shown that the number of Pt-particles smaller than 3 nm was reduced from 40 to 5% at the cathode after operation of a PEMFC for 2200 h (operation at maximum power, overhumidified gases, 80 °C cell temperature).

To maintain a large catalyst surface for a long time, operation of the fuel cell at both constant voltages and low voltage levels is preferred, that means, higher potential levels accelerate cell degradation. For example, if one considers automotive applications high potentials during sitting of the stack at stoplights or during idling occur and accelerate particle growth. Cell voltages during rapid shutdown of the stack are even higher and hence more harmful [46].

Particle redistribution can be explained with potential cycling. It is believed that platinum-solubility is a function of the potential and that there exists a particular equilibrium voltage. When the cell is cycled above the equilibrium voltage Pt-ions are driven into the solution (water). When decreasing the cycling potential again below the equilibrium, the platinum is forced back out of the solution onto the catalyst surface again [7,46,55]. Step changes in the cell voltage may also help this process [18].

(ii) Different cell temperatures during operation also have an impact on the ECSA. Generally, kinetics goes up with increasing temperature and hence higher temperatures result in faster growth of Pt-particles [7,46,54]. This is shown in Table 4.

(iii) The humidification level of the incoming reactants affects the growth of the catalyst particles as well. The lower the relative humidity (RH) of the gases, the less is the growth of the catalyst particles, especially during potential cycling. Low RH helps the lifetime of the catalyst. Table 4 shows the particle-size as a function of RH.

The catalyst loading, that is the density of Pt-particles, is believed to have no further influence on particle growth or corrosion [7,46,54]. However, according to the paper of Boyer et al. [57] the loading has at least an influence on the cell output. At a fixed cell potential of 0.7 V an increase of the loading from 0.03 to 1 mg Pt cm^{-2} results in a 200% increase of the current density to a final value of around 1.5 A cm^{-2} (H_2/O_2: 50 °C, p = atm).

Another important factor influencing the ECSA degradation is the starting surface of the catalyst which highly affects the amount of dissolved platinum. For example an initially oxidized platinum surface results in a higher amount of dissolved Pt-ions than a reduced catalyst surface. Thus, in order to obtain for instance comparable experimental data one should also take the starting condition of the Pt-catalyst layer into account [18].

Table 5 provides a quick overview of literature and operating conditions on electrocatalyst degradation.

3.1.2. Anode corrosion

The anode catalyst is much less susceptible to corrosion than the cathode catalyst. Various long-term experiments in independent works show the anode to be almost unaffected by platinum agglomeration/sintering, dissolution and oxidation, irrespective of the conditions (constant voltage or cycling) at which the fuel cell was operated [7,46,55].

Only in extended fuel cell testing after long operation periods anode catalyst deterioration can be observed. Platinum agglomeration does not occur, although the ECSA decreases. One reason might be the detachment from the carbon layer and loss of Pt-particles. Another reason may be the loss of ionomer in the catalyst (Pt-particles which are not well-bound to the carbon support move in the ionomer and can be lost easier than well-bound particles [7,58]).

3.2. Corrosion of the gas diffusion layer (GDL)

To this day much less research work has been done on the field of carbon corrosion than on the electrode catalysts. But it is known that besides the catalyst particle growth which leads to ECSA loss, carbon corrosion of the gas diffusion layer has a negative influence on the catalyst properties and subsequently on the output voltage and performance of the cell. Since carbon paper or cloth often serves as the support for the catalyst, car-

Table 5
Literature overview of electrocatalyst degradation

Authors	Experimental setup/testing conditions	Initial ECSA (%)	Loss of catalyst	Comments
Borup et al. [7]	RH 100%, 850 h, 2550 cycles	~90	No	
	RH 100%, 1500 cycles (0.1–0.75 V)	~84	No	
	RH 100%, 600 cycles (0.1–1.2 V)	~37	No	
	RH 100%, 1500 cycles (0.1–1.2 V)	~12	No	
Borup et al. [46]	H_2 RH 224%, O_2 RH 100%, 1500 cycles (0.1–1.2 V)	~61	No	ECSA strongly correlates with # of cycles
Li et al. [54]	2500 cycles (0.1.2 V)	~0.3–0.56		ECSA decrease correlated with carbon weight loss, cycling to high voltages cause high ECSA loss
	2500 cycles (0–1.0 V)	~0.68–0.74		
	Pt on Vulcan, 2500 cycles (0–1.2 V)	~30		
Wang et al. [18]	Cathode: ~1.0 A cm^{-2}, 0.64 V 1000 h	(~0.68) from 25 to 17 m^2 g^{-1}	Partly (diffusion in other electrochemically inactive parts)	Loss of Pt due to oxidation and dissolution
Wilson et al. [56]	Overhumidified gases, T_{cell} = 80 °C, 2200 h	Reduction of particles smaller than 3 nm from 40 to 5%		

bon corrosion directly affects lifetime of the cell [54]. With lost carbon, the bound platinum can also be lost [55].

(i) Potential cycling, particularly on a high level and high constant voltages exacerbate the loss of carbon material and therefore the cell lifetime [7,59].
(ii) Lower relative humidity of reactant gases aggravates the loss of carbon over time [7]. In experiments and subsequent analysis it was observed that an increase of small pore volumes happens which is believed to be caused by loss of carbon material from the micro-porous GDL. But regarding humidification of the GDL one needs to look at it accurately. In general, the water management is handled by the GDL. If we look at the performance of the cell in terms of humidity, it can be attributed to the performance of the GDL. New GDLs are usually treated to be hydrophobic to facilitate water removal and improve gas diffusion, that is, they are optimized for high relative humidity. But over time they lose the hydrophobicity which in turn reduces the mass transport rate of the gas. Higher hydrophilicity (lower hydrophobicity) means that more water tends to stay in the GDL blocking the pores and hinders transport of reactant gas molecules. This leads to a performance loss [7,46,54].
(iii) The literature is in disagreement on the influence of the operating temperature on the GDL corrosion. The reason may be different experimental setups or testing conditions. Experiments of the Los Alamos National Laboratory [7] show that temperature does not affect carbon corrosion, however this might only apply to this certain experimental setup. Li et al. [54] have monitored the carbon weight loss (gas-phase corrosion) at steady fuel cell operation with humidified air at different temperatures. For example, in accelerated tests at an air temperature of 120 °C a carbon weight loss of 8% and at 150 °C a loss of around 36% after 125 h could be observed (carbon support: Vulcan). A correlation between carbon corrosion and loss of the catalyst surface (Vulcan/Pt) area was also shown. At 0% carbon weight loss of the Pt-surface area was about 40 m^2 g^{-1} Pt. This value was reduced to around 15 m^2 g^{-1} Pt at a carbon weight loss of about 65% [54].

3.3. Chemical and mechanical degradation of the membrane

Degradation of the membrane is probably among the main factors reducing the lifetime of PEM fuel cells. Chemical stability of the membrane is critical to fuel cell's long life. Nowadays, DuPont's Nafion® and Gore's Primea® series are two of the mostly used ion exchange membranes and are considered as the industrial standard [60]. For example, Nafion® consists of a thermoplastic resin which, due to its perfluorinated composition, is relatively stable both chemically and thermally [61]. It has been shown that Nafion-type membranes are long-lasting while being used for ion exchange or electrolysis. They can reach lifetimes of several thousands of hours [5]. However, for application in PEM fuel cells they are more vulnerable and degrade more rapidly, especially in automotive applications during potential cycling, during start-up and shut-down phases as well as in freezing periods when exposed to sub-zero temperatures [5].

It is widely understood that the degradation of the membrane is a complicated multi-step mechanism, which can lead to catastrophic failure when operating the fuel cell for an extended period of time. The two major steps are (i) formation of hydroxyl (OH) and peroxyl (OOH) radicals stemming from hydrogen peroxide (H_2O_2). They chemically attack the polymer end groups that are present in the membrane [53,62]. (ii) The chemical attack along with the transient operating conditions such as potential, temperature and humidification cycling causes mechanical degradation and a change in membrane properties [53,62–64].

Many researchers are unanimous in believing that the chemical attack caused by radicals initiates membrane degradation [5,53,62,65]. Due to their unpaired electrons, the highly reactive

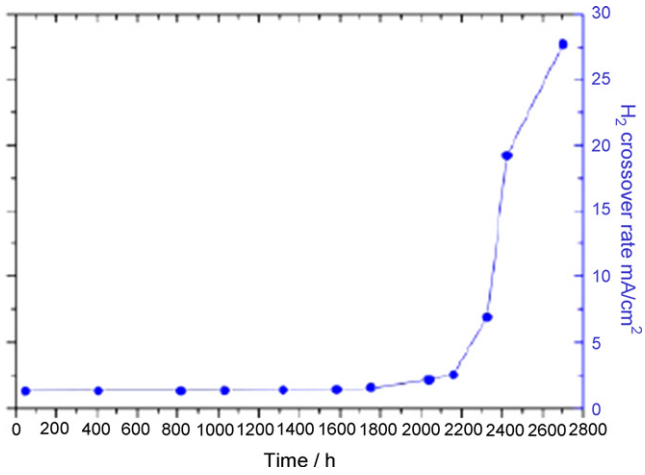

Fig. 3. H_2-crossover rate (Nafion® 112, cell temperature 75 °C, humidifier temperature of H_2/N_2 70/70 °C, gas pressure H_2/N_2 1 atm, flow rate H_2/N_2 90/370 mL min^{-1}). (Reproduced from [41] by permission of ECS – The Electrochemical Society).

and short-dated radicals react with the weak polymer endgroups of the membrane [62]. The detrimental reaction of radicals with polymer endgroups is most severe at lower humidification states and higher temperatures of around 90 °C and above [62]. Hübner and Roduner [65] observed that the peroxide radical attack is catalyzed by metal ions derived from corroded components of the MEA. The radicals originate from hydrogen peroxide which can be formed prior to the water formation. Hydrogen peroxide can be formed both at the anode and the cathode. At the anode H_2O_2 is formed when crossover of oxygen from the cathode occurs [62,64]. Also, air bleed in presence of carbon monoxide (from the fuel) at the anode can provide the oxygen to form hydrogen peroxide. At the cathode H_2O_2 can be formed in the oxygen-reduction reaction prior to the formation of water [5].

Over time the chemical attack leads to membrane degradation and thinning, both facilitating reactant gas crossover (Fig. 3) which in turn facilitates the formation of hydrogen peroxide. Fig. 4 shows a cracked membrane/MEA after long-term operation. The reason for a higher gas crossover rate can be the loss of membrane material [46]. Given that hydrogen peroxide formation occurs at both the anode and cathode as stated above, mixed potentials at both electrodes increase deterioration of the cell performance [41,67]. Mixed potentials can arise at both electrodes, when H_2 and O_2 travel through the membrane into their respective reverse electrodes and react with the other reactant [41]. These adverse reactions counteract the regular reactions taking place at the electrodes. Since this reaction is highly exothermic, the released energy may cause hot spots on the membrane surface resulting in pinhole formation. Pinholes again make gas crossover easier and subsequently a destructive cycle of increasing gas crossover and pinhole formation is established.

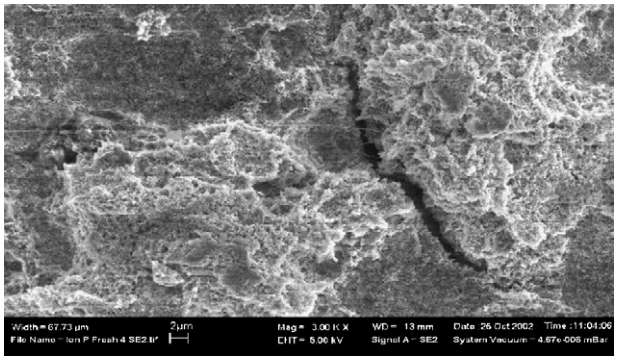

Fig. 4. Image of a cracked membrane/MEA. (Reproduced from [66] with permission from Elsevier).

Hot spots can also affect the Pt-catalyst. High temperatures usually accelerate kinetics and therefore aid Pt-sintering [41] (hot spots do not necessarily have to be understood in terms of temperature, but they can also indicate regions in the membrane with high reaction density and high current densities respectively). Furthermore, the membrane starts to lose its hydrophilicity in this process, resulting in lower conductivity of the membrane due to lower water content and therefore again loss of cell performance over time.

Also, fluoride which is initially part of the membrane polymer structure is dissolved and can be found as fluoride ions in the exiting water, which indicates a chemical change in the membrane. The concentration of lost fluoride is a good indicator for both the degradation state and the expected life [53,62,68].

The aforementioned potential-, temperature- and humidification-changes also shorten lifetime. Localized stresses can appear which promote cracks and crack enlargement which in turn facilitate the gas crossover process [53,69,40]. Liu et al. [69] observed that mechanically reinforced membranes may not suffer from the rapid and unpredictable failures which arise from hydrogen crossover, instead the degradation process for reinforced membranes is gradual which is more desirable.

In order to extend Nafion®-type polymer membrane durability research in two main areas is underway. The goal is to achieve higher chemical and mechanical stability. To impart a more stable chemical structure it is preferable among other things to remove the reactive weak endgroups in the polymer [62]. Curtin et al. showed that a reduction of the reactive polymer endgroups of the membrane is associated with a reduction of the fluoride ion release, a good life indicator as mentioned above. In experiments a chemically modified Nafion®-membrane showed about 40% less fluoride emissions in comparison to a standard Nafion® polymer in the same amount of time (50 h) [62]. Mechanical stability can be achieved by higher mechanical strength and reinforced membranes [69,70]. Liu et al. [69] illustrate that some mechanical reinforced membranes exhibited a lifetime of an order of magnitude higher than non-reinforced membranes of the same thickness. For instance, a particular reinforced membrane compared to Nafion® 101 showed a lifetime which was twice as long; the reinforced membrane in comparison to the thicker Nafion® 1035 showed a slightly longer life [69].

3.4. Corrosion and mechanical degradation of the bipolar plates and gaskets

Corrosion of the bipolar plates also impacts performance and life of a fuel cell. Three major degradation mechanisms have

been observed: (i) under permanent water contact, material of the plates dissolves and either is flushed away or travels into the membrane. The corrosion product staying in the cell accumulates and can poison the membrane. A problem in terms of efficiency arises when a (ii) resistive surface layer is formed on the plates which results in a higher ohmic resistance. In addition, (iii) when high compressive pressure is used to seal the stack and ensure good conductivity, the mechanical stress may cause fracture and deformation of the bipolar plates [5].

4. Contamination of the cell

Contamination of PEM fuel cells can also have adverse effects on performance and life [5]. Contamination is the process when impurities pollute and penetrate into cell components and/or initiate chemical attack and slow down the actual reactions taking place in the cell. The contamination products originate from components inside the cell or can be transported into the cell by the reactants. As a result, metal, alkaline metal and ammonium ions, silicon and catalyst particles as well as carbon monoxide (CO), nitrogen oxides (NO_x) or sulfur dioxide (SO_2) can be present in the cell. Even trace amounts of impurities result in considerable degradation of performance [5,71,72].

4.1. Contamination of the electrodes/electrocatalyst

Carbon monoxide is harmful for the electrocatalyst. In the literature CO-contamination is often referred to as CO poisoning [47,62]. CO can be present in the hydrogen stream when the fuel is obtained by reforming liquid hydrocarbons or alcohol fuels [5,24,60,73,74]. Since a higher CO-concentration only occurs at the fuel side, poisoning only happens at the anode. Cathode poisoning has not been reported in the literature.

It was found that even amounts as small as 50 ppm of carbon monoxide are sufficient to poison the anode reaction resulting in a lower cell potential output and a lower energy conversion efficiency [59]. The basic theory behind CO-poisoning is that CO-molecules are adsorbed [5] on the platinum catalyst sites and block the hydrogen from reaching the platinum particles. Although CO-poisoning is a slow process, it can lead to a significant performance loss, that is voltage drop over time. It does not seem to have an influence on lifetime. CO-poisoning is reversible [73,75] through air bleed at the anode. During air bleed small amounts of air can burn the CO in presence of hydrogen. While only a small amount of hydrogen is burned carbon monoxide is converted to carbon dioxide [59]. Le Canut et al. [24] conducted CO-poisoning tests with a CO-concentration of 50 ppm and 100 ppm, respectively, at a current density of 0.4 A cm^{-2}. At the low concentration of 50 ppm a drop of the cell voltage from initially 0.72 V to 0.41 V could be observed in around 60 min. At the high concentration a voltage level of 0.34 V was reached after about 13 min. The CO-poisoning could be stopped by removing carbon monoxide from the reactant. With injection of air into the fuel stream (air bleed 2%), the voltage could be fully recovered. The recovery time was 40 min for the low and around 10 min for the high CO-concentration [24]. Fig. 5 shows

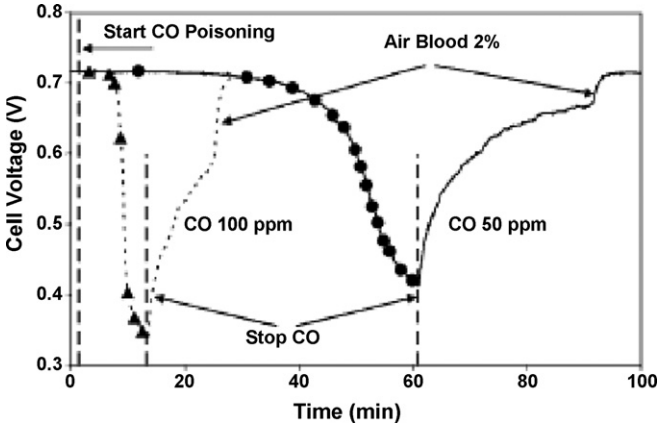

Fig. 5. Cell voltage over time for CO-poisoning of the anode, impedance tests (50 ppm CO, circles; 100 ppm CO, triangles). (Reproduced from [24] by permission of ECS – The Electrochemical Society).

the cell voltage during CO-contamination and subsequent air bleed.

4.2. Contamination of the membrane

Cationic contaminants such as alkaline metal and ammonium ions can penetrate into the membrane resulting in considerable reduction of performance [71,72]. Protons will be replaced due to the higher affinity of the cations with the sulfonic acid endgroups of the membrane, resulting in lower conductivity and water levels when the membrane is saturated in the ionomer phase as well as in a higher electro-osmotic force. This will reduce the maximum current and the exchange current density in the cells [71,72]. Kienitz et al. have shown in their model that the cationic impurities will always be more concentrated on the cathode side of the cell. They assume that the reduced performance of a contaminated cell is due to the limited proton flux at the cathode [71].

5. Reactant gas starvation

Fuel or oxidant starvation refers to the operation of fuel cells at sub-stoichiometric reaction conditions. When starved from fuel or oxygen, the fuel cell performance degrades and the cell voltage drops. In experiments Liu et al. [76] measured the polarization curves of a segmented single fuel cell with several subcells under anode and cathode starvation. During anode starvation, Liu et al. observed that the current density of the subcells nearest to the outlet (row 4 of 4) dropped immediately to zero, followed by a voltage decrease. Subsequently the current density of row 3 dropped to zero. Apparently, the subcells of rows 1 and 2 were not impacted. However lower cell potentials do not negatively influence durability; what does influence a cell's durability is a subsequent cell reversal due to starvation.

Oxygen or hydrogen starvation can result in generation of hydrogen in the cathode or oxygen in the anode. For example in the event of hydrogen starvation the cell current cannot be maintained causing a high anode potential [76]. As a result the water present at the anode may split into hydrogen and oxygen

producing oxygen in the anode:

$$2H_2O \rightarrow O_2 + 4H^+ + 4e^- \quad \text{(anode)}$$

Also, in the absence of hydrogen, the following anode reaction can take place:

$$C + 2H_2O \rightarrow CO_2 + 4H^+ + 4e^- \quad \text{(anode)}$$

Similarly during oxygen starvation the reaction at the cathode will produce hydrogen [77]. The normal cathode reaction:

$$O_2 + 4H^+ + 4e^- \rightarrow 2H_2O$$

changes to

$$2H^+ + 2e^- \rightarrow H_2 \quad \text{(cathode)}$$ [76, 77].

The presence of oxygen at the anode and hydrogen at the cathode will lead to reversal of the cell potential, that is a negative potential difference between the anode and the cathode [26]. Cell reversal accelerates corrosion of carbon components such as the backing layers with ensuing electrocatalyst corrosion and eventually leads to damaged components [76–78]. During hydrogen starvation, oxygen at the anode can react with the carbon present in the gas diffusion and backing layers to form carbon dioxide (second anode reaction above) [5,76,77,79].

Several factors can cause reactant starvation. A poor water management with flooding and a poor heat management during sub-zero temperatures and cold start-ups with ice within the cell can block the pores of the gas diffusion layers. A poor gas feeding management can lead to non-uniform distribution of the reactant gases resulting in partial or complete fuel and/or oxidant starvation or in sub-stoichiometric operation in individual cells. Also, an imperfect stack and cell design with an uneven distribution of mass in the flow fields, a poor stack assembly as well as quick load demands can be reasons contributing to gas starvation [5,76].

6. Thermal management of PEM fuel cells and the impact on performance and durability

Thermal management is particularly important when the fuel cell is exposed to freezing temperatures. To this day the operation of PEM fuel cells when cycled between sub- and above-zero temperatures and at elevated temperatures as well as cold starts are not completely understood. Although a lot of research has been done in recent years, more work needs to be done to better understand degradation of performance and durability under sub-zero and elevated temperature operation [3,6,8,80,81].

6.1. Influence of freezing temperatures on durability

Exposure of a non-operating PEM fuel cell to freezing temperatures is one of the issues affecting durability. When the fuel cell is subjected to sub-zero temperatures for an extended period of time the residual water contained within the cell can freeze. This leads to thermal and mechanical stress and hence to mechanical damage of the cell components or may even cause physical breakdown. It was observed that freezing water on Nafion®-type membranes rather than the water inside the membrane leads to degradation of the MEA. Due to the different densities of water and ice (0.9998 and 0.9168 $g\,m^{-3}$, respectively) the volume of freezing water expands about 9% [82]. The repetitive cycles of ice formation on the membrane surface and melting into water can delaminate the catalyst layer from both the membrane and the gas diffusion layer [3,82,83]. The resulting mechanical damage might lead to a loss of thermal and electrical interfacial contact since the components within the cell are no longer in proper contact. He and Mench [84] correlated the ice formation on the membrane surface with its thickness and initial water content. Since the Nafion® membranes have a large freezing temperature depression (~24.5 K), the contained liquid water can flow out of the membrane and will freeze immediately on the surface and in the catalyst layer. The thicker the membrane and the higher the initial water content, the thicker will be the developing ice layer. For instance, in the case of Nafion® 112, the ice thickness is 5 μm, whereas it is about 18 μm for Nafion® 117 (water content of Nafion® = 20 $mol_{H_2O}\,(mol_{SO_3^-})^{-1}$). Also, cracking of fully hydrated membranes after several freeze/thaw cycles (from −30 to 20 °C) was observed in tests carried out by Plug Power [59]. However, the lower the hydration state of the membrane after shut-down, the less serious are the cracks. Cracks in the membrane lead to gas crossover and in turn to uncontrolled reaction between hydrogen and oxygen with subsequent pinhole formation damaging the membrane and reducing the life of the cell [83]. This process has been discussed in Section 3.3 of this paper. In the review part of the paper by Kim and Mench [85] some results show that cells which were dried during shut-down show neither observable physical damage nor electrochemical losses during freezing.

6.2. Influence of freezing temperatures on performance

In general, performance meaning the power output of PEM fuel cells decreases with decreasing temperatures, especially when the stack is operated below 0 °C [5,86]. However, when cell temperatures reach +80 °C and higher performance starts to decrease again [3,6].

6.2.1. Different experiments on performance degradation

The work of Chang et al. shows that with decreasing temperature of the liquid water in the cell from 80 to 30 °C the proton conductivity of a Nafion® membrane can decrease up to 30%, depending on the thickness and the measurement method [87]. Mukundan et al. [8] observed that the conductivity of a Nafion® membrane below 0 °C is higher, when the water content is lower. In conductivity measurements at different temperatures of Mukundan et al. Nafion® membranes showed 10 times higher conductivity at around 25 °C (0.02 $S\,cm^{-1}$) than at −30 °C (0.002 $S\,cm^{-1}$) [8]. Performance of the fuel cell can be attributed to some extent to the conductivity of the membrane. In the study of McDonald et al. experiments were carried out to understand the physical and chemical changes in the membrane (Nafion® 112)/MEA during freeze/thaw cycles [88]. After 385 cycles from 80 to −40 °C over a period of 3

months, the membranes/MEA were analyzed on ionic conductivity, structure, and ultimate strength. No catastrophic failure was observed, but the membrane structure at the molecular level seemed to have changed resulting in a different percent elongation at failure and ultimate strength as well as the ability for water take up.

In the open literature it is agreed that fuel cells cycled between sub- and above-zero temperatures (cell temperatures) for an extended period of time show strong degradation with reversible as well as irreversible damage [83].

Mukundan et al. [8] show performance loss and damage of a fuel cell under freeze/thaw cycles. In their experiments with Nafion® 112 and humidified reactants the performance decreased with each cycle from −80 to 80 °C. For example after 9 cycles the cell potential dropped from initially 0.6 to 0.5 V (at a constant current density of 1.0 A cm^{-2}). After 10 cycles the cell failed completely due to physical damage of the carbon cloth. In other tests of Mukundan et al., a different fuel cell was cycled from −40 to 80 °C. A potential loss could also be observed. After 40 cycles the cell potential dropped from initially ca. 0.57 to ca. 0.54 V at a constant current density of 0.9 mA cm^{-2} [8]. Cho et al. [82] measured the current density of a cell subjected to thermal cycling at a constant voltage of 0.6 V. After four cycles from 80 to −10 °C (measurement at 80 °C, cool down to −10 °C, 1 h at −10 °C, warm up to 80 °C for the next measurement) the current density dropped from initially 880 to 780 mA cm^{-2}. In the research paper of Mukundan et al. [89] polarization curves during freeze/thaw cycling experiments using different GDL, among other things, were obtained. It could be seen that a paper GDL performed worse than a cloth GDL. In these tests, the stack was operated at 80 °C with humidified reactants. After reactant shut-down it was subjected to 100 repeated freeze/thaw cycles from 40 to −40 °C (slow cooling within 4 h) and from 80 to −40 °C (fast cooling within 1 h). In the slow cooling experiments the cells were removed to be tested at 80 °C; when fast cooled after 10 cycles. During the slow cooling, the paper GDL showed strong degradation after 40 cycles, especially at high current densities in the mass transport region, whereas the cloth GDL showed no performance loss even after 100 cycles. For the experiments with the fast cooling (new cells prepared the same way) an even stronger degradation could be observed for the paper GDL, while the influence on the cloth GDL was little [89].

When operating in freezing conditions as with a fuel cell exposed to freezing temperatures, the MEA, the backing layers and the gas diffusion layers can be delaminated. The backing layer fibers and the binder structure as well as the gas diffusion layer itself can be damaged, too. The reason for GDL deterioration might be the relatively high water content during operation and after shut-down. Therefore the probability that freezing water can be found within the pores is high. With delamination of various component layers the thermal and electric interfacial contact is lost [3,83,90]. Basically, the same consequences as mentioned in the previous paragraph can be given. Water contained inside the membrane with strong bonds with cations does not freeze and therefore does not have an impact on performance [3,90].

6.2.2. Start-up from freezing temperatures

Another concern at sub-zero temperatures is the start-up of fuel cells. If the generated water in the cathode is not removed while the cell is running at sub-zero temperatures, ice will form causing voltage drop and even shuts down the electrochemical reaction. This is more likely to happen at higher current densities. Therefore it is important that before ice completely blocks the catalyst layer the cell temperature reaches above freezing [91,92]. Ge and Wang [93] studied liquid water and ice formation on the surface of the catalyst layer during cold start at different freezing temperatures (−5, −3 and −1 °C). Before the cold start with dry reactants the cell was purged for 2 min and the current density was set to 0.02 A cm^{-2}. Throughout the whole cold start no water drops or ice on the surface of the "catalyst-coated membrane" (CCM) was observed which shows that purging the cell prior to start is beneficial during cold starts. Tajiri et al. conducted a test on isothermal start-up of fuel cells from −30 °C. They show that the membrane is the critical component for improving the performance during isothermal cold start [94]. Khandewal et al. [95] also studied cold start behavior and the corresponding energy requirement of PEM fuel cells using a one-dimensional thermal model. They observed that there is a range of current density in which the cell can be started optimally from freezing temperatures. The simulation shows that a current density of 0.1 A cm^{-2} is not enough to bring the stack from −20 to above 0 °C in order to reach the start-up condition, whereas at 1.0 A cm^{-2} the stack needed around 69 s (neither heated coolant flow was used nor initial ice was present). The start-up time of 69 s could be reduced significantly to 20 s, when the fuel was heated from −20 to around 0 °C. Interestingly, heating the reactant gas at the cathode did not contribute much to a faster start-up. Additionally, heated endplates of the stack is recommended to achieve a rapid start-up. Ahluwalia and Wang [91] observed that the current density during cold start needs to be limited in order to prevent continuous voltage decrease until shut-down of the electrochemical reaction due to freezing water. In experiments (isothermal) and in calculations ice is formed only when the current density exceeds a certain value. For example, during start-up from −25, −20 and −10 °C, the maximum current density was determined to be less than 1, 3 and 10 A cm^{-2}, respectively (pressure = 1 atm, flow rate L min^{-1}: H_2 0.66 (−25 °C), 1.19 (−20 °C) and 0.79 (−10 °C); O_2 2.83, 9.49 and 6.33).

6.3. Influence of elevated temperatures on performance and lifetime

Operation of fuel cells under higher temperatures (>100 °C) has a few advantages [81]: the electrochemical kinetics and hence the efficiency improves, the tolerance for contaminants increases and water management and cooling are enhanced due to a higher temperature difference between the cell and the coolant. Waste heat can be recovered, CO-poisoning is reduced and therefore lower quality hydrogen from reformation can be used [81,96]. Despite the various advantages of operating the fuel cell at higher temperatures the degradation of cell components will be accelerated and longtime performance and durability are expected to decrease [81,96–98].

While even at moderate temperatures the degradation of the electrodes/electrocatalyst and growth and loss of its (Pt-) particles is a concern [5,7,46], at higher temperatures the chemical (in)stability of the catalyst is of even higher importance as redistribution, sintering and agglomeration of the particles are accelerated [51,96,98]. This process was described in detail when we discussed corrosion of the electrodes and electrocatalyst. A second issue at elevated temperature operation can arise if the potential at the cathode is held high. This initiates the split of the oxygen molecule into oxygen atoms, which, at a high temperature, can react easily with carbon and/or water to form CO and CO_2 resulting in carbon corrosion [81]. This in turn causes catalyst degradation which affects lifetime [54].

At elevated temperature operation the water uptake of the membrane can be aggravated and proton conductivity may decrease, especially at low relative humidities. This leads to a significant resistive loss lowering the cell performance and efficiency [97]. For example, Song et al. studied the effect of Nafion® content on electrode performance under three different temperatures (80, 100 and 120 °C). They observed that the influence of the Nafion content at 120 °C was larger than at the lower temperatures, meaning that the content needs to be taken into account during elevated temperature operation. In the case of non-optimized Nafion® content a mass transport problem was observed which resulted in lower performance [97].

7. Conclusions

This paper provided a brief overview of the main parameters influencing performance and durability of PEM fuel cells. Various interacting mechanisms contribute to loss of performance and negatively impact fuel cell durability. It is important to understand these processes and interactions well to take the necessary steps to extend the life of next-generation fuel cells. We hope that this paper is a step towards understanding the vast but spread-out work that has been done and reported in the literature on fuel cell performance and durability; and help identify critical directions for further research. A summary of some of the key points is given below.

Cycled operation of the fuel cell is much more detrimental to lifetime than operation at constant load. Poor water management can cause flooding, while flooding reduces the electrochemical active surface area (ECSA) as well as corrosion or degradations of the electrodes, the catalyst layers, gas diffusion media and the membrane. The loss of ECSA results in lower activity of the catalyst and hence in lower power output. It does not lead to failure of the cell. Corrosion products can contaminate the cell; however this does not seem to have a big impact on fuel cell performance and life. CO-poisoning can hinder or slow down the reaction at the anode leading to lower cell potentials, but it is a reversible process. Membrane contamination mainly results in lower performance.

Robustness of the membrane is critical to durability of PEM fuel cells. In particular carbon corrosion and change of the chemical structure of the membrane can seriously compromise durability. During membrane corrosion, pinholes may be formed leading to gas crossover through the membrane. Also dehydration, mostly at the anode side of the membrane can occur which may lead to lower conductivity in the short term and brittleness in the long term. Membrane cracking is possible leading again to gas crossover, hot spots and pinhole formation, a subsequent destructive cycle leads to cell failure.

Operation or even storage of fuel cells at freezing temperatures results in internal thermal and mechanical stresses, cracks in the membrane, delamination of the component layers and loss of electrical contact, all negatively influencing fuel cell performance and life. Operation at elevated temperatures aggravates degradation mechanisms such as corrosion.

Since a fuel cell stack is a complex system consisting of electrodes, membrane, gas diffusion layers and other components fuel cell life depends on individual components as well as on the interaction of all parts. Degradation mechanisms are interconnected and individual degradation can influence or initiate further deterioration of other components. Therefore it is difficult to quantify durability and to rank the mechanisms. However, corrosion and change in the chemical structure of the membrane might be among the most important issues during operation. Degradation of the catalysts and of other components deteriorates performance but plays a less important role in sudden cell failure.

Acknowledgements

The authors are grateful to Dr. Rui (Jim) Qiao and Dr. Pierluigi Pisu of the Department of Mechanical Engineering at Clemson University for their positive feedback. The authors would also like to thank Dr. Steve Creager from the Chemistry Department at Clemson for his input.

References

[1] G. Escobedo, M. Gummalla, R.B. Moore, DOE Hydrogen Program, FY 2006 Annual Progress Report, 2006, pp. 706–711.
[2] R. Borup, M. Inbody, J. Davey, D. Wood, F. Garzon, J. Tafoya, J. Xie, S. Pacheco, DOE Hydrogen Program, FY 2004 Annual Progress Report, 2004, pp. 579–584.
[3] Q. Yan, H. Toghiani, Y.-W. Lee, K. Liang, H. Causey, J. Power Sources 160 (2006) 1242–1250.
[4] http://www.mercedes-benz.de/content/germany/mpc/mpc_germany_website/de/home_mpc/buses/home/bus_world/whats_new/Bus_news_2005/World_record_for_fuel_cell_buses.html, 2005.
[5] G. Hinds, NPL Report DEPC-MPE 002, 2004, pp. 25–42.
[6] A. Faghri, Z. Guo, Int. J. Heat Mass Transfer 48 (2005) 3891–3920.
[7] R.L. Borup, J.R. Davey, F.H. Garzon, D.L. Wood, M.A. Inbody, J. Power Sources 163 (2006) 76–81.
[8] R. Mukundan, Y.S. Kim, F. Garzon, B. Pivovar, ECS Trans. 1 (2006) 403–413.
[9] C. Sishtla, G. Koncar, R. Platon, S. Gamburzev, J. Power Sources 71 (1998) 249.
[10] K. Washington, Proceedings Fuel Cell Seminar 2000, Portland, U.S.A., 2000, p. 468.
[11] U. Pasaogullari, C.Y. Wang, J. Electrochem. Soc. 152 (2) (2005) A380–A390.
[12] H. Maeda, A. Yoshimura, H. Fukumoto, Proceedings Fuel Cell Seminar 2000, Portland, U.S.A., p. 379.
[13] M. Fowler, J.C. Amphlett, R.F. Mann, B.A. Peppley, P.R. Roberge, J. New Mat. Electrochem. Syst. 5 (2002) 255.

[14] E. Endoh, S. Terazono, H. Widjaja, Abstract 89, Electrochem. Soc. Meeting Abstracts, Salt Lake City, U.S.A., 2002.
[15] S.D. Knights, K.M. Colbow, J. St-Pierre, D.P. Wilkinson, J. Power Sources 127 (2004) 127–134.
[16] J. Scholta, N. Berg, P. Wilde, L. Jorissen, J. Garche, J. Power Sources 127 (2004) 206–212.
[17] X. Cheng, L. Chen, C. Peng, Z. Chen, Y. Zhang, Q. Fan, J. Electrochem. Soc. 151 (2004) A48–A52.
[18] X. Wang, D. Myers, R. Kumar, Proceedings of the Fuel Cells Durability, first ed., Washington, DC, 2006, pp. 151–162.
[19] V. Lightner, DOE Hydrogen Program, Record 5036, 2006.
[20] V. Lightner, DOE Hydrogen Program, Backup Ref. 5036a, 2006.
[21] R. Borup, D. Wood, J. Davey, P. Welch, F. Garzon, DOE Hydrogen Review, Presentation, 2006.
[22] R. Borup, D. Wood, J. Davey, P. Welch, F. Garzon, DOE Hydrogen Review, FY 2006 Annual Progress Report, 2006.
[23] S.J.C. Cleghorn, D.K. Mayfield, D.A. Moore, J.C. Moore, G. Rusch, T.W. Sherman, N.T. Sisofo, U. Beuscher, J. Power Sources 158 (2006) 446–454.
[24] J. Le Canut, R.M. Abouatallah, D.A. Harrington, J. Electrochem. Soc. 153 (2006) A857–A864.
[25] I. Manke, N. Kardjilov, A. Haibel, C. Hartnig, M. Strobl, A. Rack, A. Hilger, J. Scholta, W. Lehnert, W. Treimer, S. Zabler, J. Banhart, DGZfP-Berichtsband 94-CD, 2005.
[26] T. van Nguyen, M.W. Knobbe, J. Power Sources 114 (2003) 70–79.
[27] T.V. Nguyen, R.E. White, J. Electrochem. Soc. 140 (1993) 2178–2186.
[28] W. He, G. Lin, T.V. Nguyen, AICHE J. 49 (2003) 3221–3228.
[29] D.A. McKay, W.T. Ott, A.G. Stefanopoulou, Modeling, parameter identification, and validation of reactant water dynamics for a fuel cell stack, in: Proceedings of the IMECE, ASME Int. Mech. Eng. Congress & Exposition, 2005.
[30] B.A. Dipierno, M.H. Fronk, US Patent 6,103,409 (2000).
[31] A.Z. Weber, R.M. Darling, J. Newman, J. Electrochem. Soc. 151 (10) (2004) A1715–A1727.
[32] A. Turhan, K. Heller, J.S. Brenizer, M.M. Mench, J. Power Sources 160 (2006) 1195–1203.
[33] J.J. Kowal, A. Turhan, K. Heller, J.S. Brenizer, M.M. Mench, J. Electrochem. Soc. 153 (2006) A1971–A1978.
[34] J. St-Pierre, D.P. Wilkinson, S. Knights, M. Bos, J. New Mat. Electrochem. Syst. 3 (2000) 99–106.
[35] Y. Wang, C.-Y. Wang, Electrochim. Acta 51 (2006) 3924–3933.
[36] S. Ge, C.-Y. Wang, J. Electrochem. Soc. 154 (2007) B998–B1005.
[37] Y. Sone, P. Ekdunge, D. Simonsson, J. Electrochem. Soc. 143 (1996) 1254.
[38] F.N. Büchi, S. Srinivasan, J. Electrochem. Soc. 144 (1997) 2767.
[39] G. Li, P.G. Pickup, Electrochem. Solid-State Lett. 9 (2006) A249–A251.
[40] X. Huang, R. Solasi, Y. Zou, M. Feshler, K. Reifsnider, D. Condit, S. Burlatsky, T. Madden, J. Polym. Sci. Part B Polym. Phys. 44 (16) (2006) 2346–2357.
[41] J. Yu, T. Matsuura, Y. Yoshikawa, M.N. Islam, M. Hori, Electrochem. Solid-State Lett. 8 (2005) A156–A158.
[42] N.E. Vanderborgh, J.R. Huff, J. Hedstrom, IEEE CH2781-3/89/0000-163 (1989) 1637–1640.
[43] T. Nguyen, J. Hedstrom, N. Vanderborgh, in: R.E. White, A.J. Appleby (Eds.), The Electrochem. Soc. Softbound Proceedings Series PV 89–14 (1989) 39.
[44] T.E. Springer, J. Zawodzinski, S. Gottesfeld, in: R.E. White, M.W. Verbrugge, J.F. Stockel (Eds.), The Electrochem. Soc. Softbound Proceedings Series PV 91–10 (1991) 209.
[45] P.J. Schutz, in: R.E. White, A.J. Appleby (Eds.), The Electrochem. Soc. Softbound Proceedings Series PV 89–14 (1989) 87.
[46] R.L. Borup, J.R. Davey, F.H. Garzon, D.L. Wood, M.A. Inbody, Proceedings of the Fuel Cells Durability, first ed., Washington, DC, 2006, pp. 21–42.
[47] P. Meyers, R.M.S. Darling, The Electrochem. Soc. Meeting Abstracts, Abstract 1212, Paris, France, 2003.
[48] S. Motupally, T.D. Jarvi, The Electrochem. Soc. 208th Meeting, Abstract, Los Angeles, CA, 2005.
[49] C. Paik, T. Skiba, V. Mittal, S. Motupally, T. D. Jarvi, The Electrochem. Soc. 207th Meeting, Abstract 771, Quebec City, Canada, 2005.
[50] T. Patterson, Effect of potential cycling on loss of electrochemical surface area of platinum catalyst in polymer electrolyte membrane fuel cell, in: AICHE National Conference, New Orleans, LA, 2002.
[51] M.S. Wilson, F.H. Garzon, K.E. Sickafus, S. Gottesfeld, J. Electrochem. Soc. 140 (1993) 2872–2877.
[52] P. Ascarelli, V. Contini, R. Giorgi, J. Appl. Phys. 91 (2002).
[53] G. Escobedo, K. Schwiebert, K. Raiford, G. Nagarajan, F. Principe, Proceedings of the Fuel Cells Durability, first ed., Washington, DC, 2006, pp. 83–100.
[54] W. Li, M. Ruthkosky, M. Balogh, R. Makharia, S. Oh, Proceedings of the Fuel Cells Durability, first ed., Washington, DC, 2006, pp. 101–114.
[55] A. Horky, K. Beverage, O. Polevaya, Y. Shi, Proceedings of the Fuel Cells Durability, first ed., Washington DC, 2006, pp. 133–150.
[56] M.S. Wilson, F.H. Garzon, K.E. Sickafus, S. Gottesfeld, J. Electrochem. Soc. 140 (1993) 2872.
[57] C. Boyer, S. Gamburzev, O. Velev, S. Srinivasan, A.J. Appleby, Electrochim. Acta 43 (1998) 3703–3709.
[58] K.L. More, K.S. Reeves, 2005 DOE Hydrogen Program Review, Arlington, VA, 2005.
[59] Z. Qi, Proceedings of the Fuel Cells Durability, first ed., Washington, DC, 2006, pp. 163–190.
[60] K. Duff, Stainless Steel alloys for Polymer Electrolyte Membrane (PEM) Fuel Cells, presentation, 2005, http://www.chemistry.oregonstate.edu/courses/ch407h/CH407H%20project%20keegan%20fuel%20cell%20steels.ppt.
[61] J. Larminie, A. Dicks, Fuel Cell Systems Explained, John Wiley & Sons Ltd., Chichester, England, 2003.
[62] D.E. Curtin, R.D. Lousenberg, T.J. Henry, P.C. Tangeman, M.E. Tisack, J. Power Sources 131 (2004) 41–48.
[63] F. Finsterwalder, M. Quintus, M. Schaloske, T. Guth, G. Frank, The Electrochem. Soc. 210th Meeting, Abstract 0485, Cancun, Mexico, 2006.
[64] V.O. Mittal, H.R. Kunz, J.M. Fenton, Abstract 0448, The Electrochem. Soc. 210th Meeting, Cancun, Mexico, 2006.
[65] G. Hübner, E. Roduner, J. Mater. Chem. 9 (1999) 409–418.
[66] S. Kundu, M.W. Fowler, L.C. Simon, S. Grot, J. Power Sources 157 (2006) 650–656.
[67] V. Ramani, H.R. Kunz, J.M. Fenton, The Electrochem. Soc. Interf. 17–19 (2004) 45.
[68] R. Baldwin, M. Pham, A. Leonida, J. McElroy, T. Nalette, J. Power Sources 29 (1990) 399–412.
[69] W. Liu, K. Ruth, G. Rusch, J. New Mat. Electrochem. Syst. 4 (2001) 227–231.
[70] Q. Li, R. He, J.O. Jensen, N.J. Bjerrum, J. Am. Chem. Soc., Chem. Mater. 15 (2003) 4896–4915.
[71] B. Kienitz, H. Baskaran, B. Pivovar, T. Zawodzinski Jr., ECS Trans. 11 (2007) 777–788.
[72] X. Cheng, Z. Shi, N. Glass, L. Zhang, J. Zhang, D. Song, Z.-S. Liu, H. Wang, J. Shen, J. Power Sources 165 (2007) 739–756.
[73] A. Rodrigues, J.C. Amphlett, R.F. Mann, B.A. Peppley, P.R. Roberge, Proceedings of the 32nd Intersociety Energy Conversion Engineering Conference, IECEC-97 (1997) 768–773.
[74] D.D. Penta, K. Bencherif, Q. Zhang, M. Sorine, Proceedings of the 2006 IEEE Int. Conference on Control Applications, Munich, Germany, 2006.
[75] J.J. Baschuk, X. Li, Int. J. Energy Res. 25 (2001) 695–713.
[76] Z. Liu, L. Yang, Z. Maoa, W. Zhuge, Y. Zhang, L. Wang, J. Power Sources 157 (2006) 166–176.
[77] D.P. Wilkinson, J. St-Pierre, PEM fuel cell durability, in: W. Vielstich, H. Gasteiger, A. Lamm (Eds.), Handbook of Fuel Cells – Fundamentals, Technology and Applications, Fuel Cell Technology and Applications, vol. 3, John Wiley and Sons, 2003.
[78] T.W. Patterson, R.M. Darling, Electrochem. Solid-State Lett. 9 (2006) A183–A185.
[79] M. Saito, K. Hayamizu, T. Okada, J. Phys. Chem. 109 (2005) 3112–3119.
[80] M. Sundaresan, R.M. Moore, J. Power Sources 145 (2005) 534–545.
[81] J. Zhang, Z. Xie, J. Zhang, Y. Tang, C. Song, T. Navessin, Z. Shi, D. Song, H. Wang, D.P. Wilkinson, Z.S. Liu, S. Holdcroft, J. Power Sources 160 (2006) 872–891.

[82] E. Cho, J. Ko, H.Y. Ha, S. Hong, K. Lee, T. Lim, I. Oh, J. Electrochem. Soc. 150 (2003) A1667–A1670.
[83] A. Pesaran, G.-H. Kim, J. Gonder, Proceedings of the Fuel Cells Durability, first ed., Washington, DC, 2006, pp. 205–227.
[84] S. He, M.M. Mench, J. Electrochem. Soc. 153 (9) (2006) A1724–A2173.
[85] S. Kim, M.M. Mench, J. Power Sources 174 (2007) 206–220.
[86] F. Kagami, F. Ogawa, Y. Hishinuma, T. Ghikahisa, Fuel Cell Seminar 2002, Palm Springs, USA, 2002, p. 239.
[87] C.H. Lee, H.B. Park, Y.M. Lee, R.D. Lee, Ind. Eng. Chem. Res. 44 (2005) 7617–7626, Sources 165 (2007) 739–756.
[88] R.C. McDonald, C.K. Mittelsteadt, E.L. Thompson, Fuel Cells 4 (3) (2004) 208–213.
[89] R. Mukundan, Y.S. Kim, T. Rockward, J.R. Davey, B. Pivovar, D.S. Hussey, D.L. Jacobson, M. Arif, R. Borup, ECS Trans. 1 (2007) 543–552.
[90] Y. Hishinuma, T. Chikahisa, F. Kagami, T. Ogawa, JSME Int. J. B 47 (2004) 235–241.
[91] R.K. Ahluwalia, X. Wang, J. Power Sources 162 (2006) 502–512.
[92] L. Mao, C.-Y. Wang, J. Electrochem. Soc. 154 (2007) B139–B146.
[93] S. Ge, C.Y. Wang, Electrochem. Solid-State Lett. 9 (11) (2006) A499–A503.
[94] K. Tajiri, Y. Tabuchi, C.Y. Wang, J. Electrochem. Soc. 154 (2) (2007) B147–B152.
[95] M. Khandelwal, S. Lee, M.M. Mench, J. Power Sources 172 (2007) 816–830.
[96] A.S. Arico, A. Stassi, E. Modica, R. Ornelas, I. Gatto, E. Passalacqua, V. Antonucci, ECS Trans. 3 (2006) 765–774.
[97] Y. Song, H. Xu, Y. Wei, H.R. Kunz, L.J. Bonville, J.M. Fenton, J. Power Sources 154 (2006) 138–144.
[98] W. Bi, T.F. Fuller, Abstract 395, The Electrochem. Soc., 212th ECS Meeting, Washington, DC, 2007.